Biochimica et Biophysica Acta, 459 (1977) 578–595

BBA 47258

POLARIZATION OF FLUORESCENCE FROM SINGLE SKINNED GLYCERINATED RABBIT PSOAS FIBERS IN RIGOR AND RELAXATION

JULIAN BOREJDO and SUSAN PUTNAM

Cardiovascular Research Institute, University of California, San Francisco, Calif. 94143 (U.S.A.)

(Received September 3rd, 1976)

SUMMARY

Single skinned glycerinated muscle fibers were labelled with the fluorescent dye *N*-(iodoacetylamino)-1-naphthylamine-5-sulfonic acid (1,5-IAEDANS). The heavy chain of myosin (EC 3.6.1.3) was labelled predominantly when the reaction was carried out in relaxation at 0 °C. Mechanical properties of skinned fibers were little affected by labelling with the fluorophore. Rigor tension developed upon transferring native or labelled skinned fibers from relaxing to rigor solutions lacking Ca^{2+} was very small but could be enhanced by progressively increasing Ca^{2+} concentration; the rigor tension decreased with increasing sarcomere length.

Polarization of fluorescence of skinned fibers reacted with 1,5-IAEDANS was measured along the line of excitation as well as at 90 ° to it. The mean values of parallel and perpendicular components of polarization of labelled fibers measured at 0° were close to the values obtained for native fibers irrigated with 1,5-IAEDANS-labelled heavy meromyosin, fiber "ghosts" irrigated with labelled heavy meromyosin, and oriented bundles of myofibrils reacted with the same fluorophore. Skinned fibers stretched above the rest length and then irrigated with 1,5-IAEDANS-labelled heavy meromyosin gave rise to polarized fluorescence close to the values theoretically predicted for an assembly of helically arranged fluorophores. Using 90° detection system a satisfactory fit to the theory could be obtained from single fibers labelled with 1,5-IAEDANS and measured in rigor. The angle between the fiber axis and the direction of the emission dipole of 1,5-IAEDANS attached to subfragment-1 was estimated to be near 40°.

INTRODUCTION

A series of investigations centering around measurements of polarized fluorescence emitted by muscle fibers excited with polarized light began with the discovery by

Abbreviations: 1,5-IAEDANS, *N*-(iodoacetylamino)-1-naphthylamine-5-sulfonic acid; MalNEt, *N*-ethylmaleimide; EGTA, ethyleneglycol-bis-(β-aminoethylether)-*N*,*N*'-tetraacetic acid; SDS, sodium dodecyl sulfate.

Aronson and Morales [1] that the physiological state of muscle can be distinguished by such measurements. Subsequently Dos Remedios et al. [2] suggested that the changes in the polarization of the intrinsic tryptophan fluorescence result from alterations in the orientation of the myosin subfragment-1 with respect to actin. More recently, Nihei et al. [3] initiated the study of the same effects arising from the fluorescence of an extrinsic fluorophore, *N*-(iodoacetylamino)-1-naphthylamine-5-sulfonic acid (1,5-IAEDANS) believed to be covalently attached to the fast-reacting cysteine residue located in subfragment-1 of myosin (EC 3.6.1.3) [4]. The Nihei et al. [3] approach combines the advantages of a potentially selective labelling of myosin with a wide separation between excitation and emission wavelengths. Furthermore, given the specificity of 1,5-IAEDANS, it is possible to calculate the depolarization of fluorescence due to the helical arrangement of fluorophores (subfragment-1-containing label) in rigor and thus to attempt to estimate the attitudinal angle of subfragment-1 with respect to the fiber axis [5]. The present work is the continuation of efforts to answer the question of whether the fluorescent dye-labelled fibers are a meaningful model for a helical array of fluorophores and so whether the polarized fluorescence can be used as a quantitative measure of the attitudinal angle of the cross-bridge. We have employed skinned glycerinated muscle preparations in the hope of reducing possible artifacts associated with the light scattering by the cell membrane. By using a new technique of labelling we have shown that in skinned fibers the majority of fluorophores are attached to myosin heavy chains without significantly affecting physiological characteristics of the muscle. Furthermore, in skinned preparations the magnitude of rigor tension developed on transition from relaxation to rigor is greatly reduced and the accompanying disorganization of sarcomere structure, which could constitute a significant source of error in polarization measurements, is eliminated. In the present work we report on the measurements of polarization of fluorescence observed both along the line of excitation and at 90° to it. While there is still a discrepancy between predicted and experimentally obtained values of parallel and perpendicular components of polarized fluorescence measured at 0°, right angle data in which the contribution of randomly oriented fluorophores is minimal, can now be interpreted with the aid of a theory that is summarized in the Appendix to this paper. Consequently the absolute attitude of myosin subfragment-1 with respect to actin axis can be estimated. Upon transition from rigor to relaxation there appears to be disorganization of the helical arrangement of the cross-bridges.

MATERIALS AND METHODS

Fiber preparation. Fibers were glycerinated according to the method of Szent-Gyorgyi [6] for a period ranging from 2 to 8 weeks. Single fibers 5–10 mm long were dissected from bundles in a solution containing 50 % (v/v) glycerol, 5 mM sodium phosphate buffer, pH 7.0. The fibers were skinned by splitting them lengthwise with a pair of sharpened jewelers tweezers as previously described [7]. The quality of the fiber was checked with Nomarski's microscope optics under 500 ×magnification and only the preparations exhibiting a regular sarcomere pattern were used in the experiments. Myofibrils were prepared [8] from rabbit psoas muscles and kept at −18 °C in 4.1 M glycerol. Shortly before the experiment the fibrils were centrifuged for 10 min at 5000×*g* and resuspended in rigor solution; the procedure was repeated three more times.

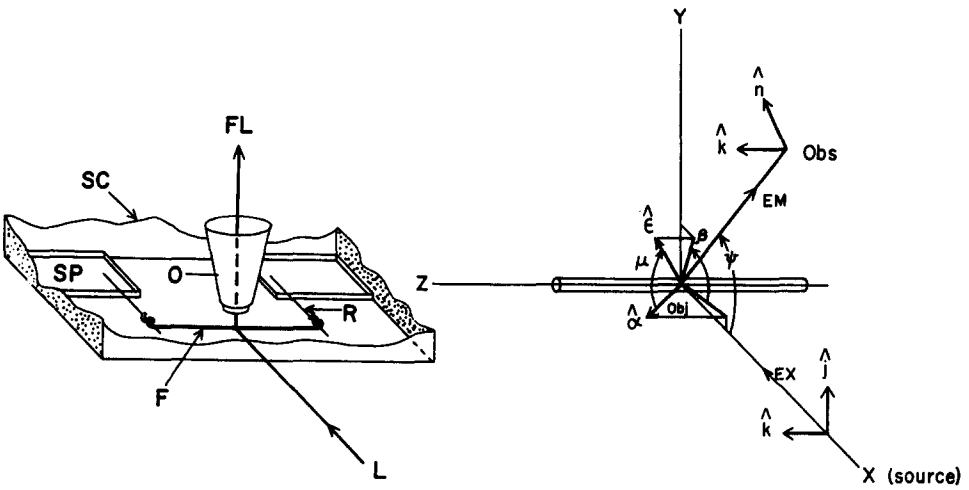

Fig. 1. Apparatus used for measuring polarization of fluorescence at right angles to the direction of the incident light. SC, Suprasil cuvette with one window removed; SP, glass slide supporting the reed R. By moving the slides apart the fiber length could be adjusted. F, muscle fiber; O, microscope objective perpendicular to the fiber axis and to the direction of the incident light L; FL, collected fluorescent light. The coordinate system used in the text is shown at right. Muscle fibers axis is parallel to the *Z* axis. Polarizer and analyzer directions lie in the *YZ* and *XZ* planes, respectively. A is an absorption and E an emission dipole.

Mechanical measurements. Measurements were performed in a quartz cell, identical to one previously described [7]. For the measurements of fluorescence at 90° to the excitation beam the muscle fiber was mounted in a Suprasil spectrophotometric cuvette which had one of the windows removed. The schematic diagram of the cell is shown in Fig. 1. One end of the skinned fiber was tied to an inextensible support and the other to a glass rod (diameter 15 μm) whose deflection was calibrated in terms of force by suspending microscopic weights at the point of muscle attachment. Com-

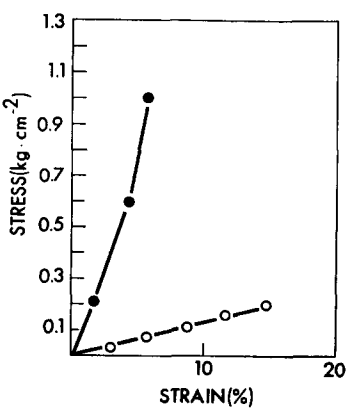

Fig. 2. Stress-strain relationship of single skinned glycerinated muscle fiber in rigor (●) and in relaxing (○) solution. The modulus of elasticity of this fiber up to 5 % strain was 0.14 and 0.013 kg/cm² in rigor and relaxing solutions, respectively. Fiber length was 316 mm and the diameter 63 μm

pliance of the glass rod was 11.2 μm/mg. Deflection was observed under 250× magnification. The static stiffness of skinned preparations measured in relaxing solution was 0.013 kg/cm^2 (Fig. 2). The maximum isometric tension ranged between 1 and 2 kg/cm^2 but could not be maintained for more than a few seconds due to the breakage. The solutions were changed by flushing the cell with a syringe arrangement which applied solution at one end of the cell and sucked it rapidly at the other. Complete change of solution could be achieved in about 10 s.

Solutions. Rigor solution contained 80 mM KCl, 5 mM $MgCl_2$, 2 mM EGTA and 5 mM sodium phosphate buffer, pH 7.0. Relaxing and activating solutions contained the same ingredients plus 5 mM ATP. Activating solution had the same composition as relaxing solution except that 0.1 mM $CaCl_2$ replaced the EGTA.

Labelling the fibers with 1,5-IAEDANS. The labelling procedure of Nihei et al. [3, 9] was modified in view of the recent findings of Duke et al. [10], viz. that in the absence of actin binding the affinity of 1,5-IAEDANS for the SH group of myosin is significantly increased and that of actin thiols is significantly decreased. Consequently, labelling was performed under the conditions where dissociation between myosin and actin is maximal, i.e. during relaxation at 0 °C. A skinned fiber was mounted at resting length in an experimental chamber and equilibrated with rigor solution for 1 h at 0 °C. The fiber was then transferred to a relaxing solution for 1 h at 0 °C and finally to a relaxing solution containing 0.069 mg/ml 1,5-IAEDANS or ^{3}H-labelled 1,5-IAEDANS for 1 h at 0 °C. The incubation was stopped by washing the fibers first with cold relaxing solution and then with rigor solution at 25 °C. Myofibrils were labelled as follows: They were first washed in relaxing solution and then in relaxing solution containing 1,5-IAEDANS. After 1 h equilibration at 0 °C they were washed with relaxing solution and twice with rigor solution.

The location of the fluorescent or radioactive label within the muscle was assessed by polyacrylamide gel electrophoresis. Fibers were dissolved in 5 μl of solution containing 1 % SDS, 6 M urea, 1 % β-mercaptoethanol and 25 % Tris/glycine buffer, pH 8.6. The samples were applied to a micro-polyacrylamide gel (1.1 × 1.1 mm; 5 % SDS) mounted in an Ortec 4200 electrophoresis apparatus, and run for 3 h at 0.5 mA per tube. A single muscle fiber (2 μg protein) was enough material to obtain a distinct band, but for greater resolution three separate skinned fibers were usually used. Immediately after the electrophoresis the gels were examined for the presence of fluorescent bands on a gel scanner (devised by R. A. Mendelson).

Myofibrils were treated in the same fashion, except that the normal size gels were used. After the electrophoresis each gel was immersed overnight in 7.5 % acetic acid and then washed for 24 h with water to remove the acid. The gels were then frozen, sliced, placed in scintillation vials, solubilized by 30 % H_2O_2 at 37 °C overnight and radioactivity was determined in Beckmann LS-150 counter [10] with an efficiency of 49–50 %.

Heavy meromyosin was reacted with 1,5-IAEDANS at 1 : 1 molar ratio of protein to reagent overnight at 0 °C. Unreacted fluorophore was then dialyzed out against a large excess of rigor solution.

Fluorescence measurement. The measurements at observation angle $\psi = \pi$ (Fig. 1) were carried out in an apparatus described earlier by Tregear and Mendelson [5] with little modification: the incident light from 75 W Xe lamp was limited by a 1 mm diaphragm and collected by a 20 × Tiyoda objective (N.A. = 0.4). In the experimental

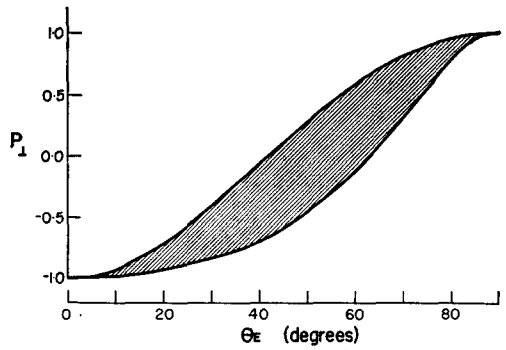

Fig. 3. The theoretical limits on the possible values of $P_\perp$ as a function of the angle between the emission dipole and fiber axis for the fluorescence detected at 90° to the direction of excitation. The corresponding curve for $P_{||}$ is given in ref. 5, Fig. 2.

arrangement for detection at $\psi = \pi/2$ the incident light beam from a 75 W xenon-mercury lamp (Illumination Industries, Sunnyvale, Calif.) was orthogonal to both the fiber axis and the axis of the analyzer (Fig. 1). Each measurement of fiber fluorescence was followed by a control measurement of the fluorescence with the fiber removed. A glass coverslip defining the top of the experimental chamber eliminated the possible ruffling of the solution surface.

The results were expressed in terms of polarizations $P_\perp$ and $P_{||}$ (see Eqns. 9 and 10 of Appendix).

The values of polarization of fluorescence measured at $\psi = \pi$ were interpreted on the basis of a formal treatment introduced by Tregear and Mendelson [5]. However, the present treatment (Appendix) extends and at one point corrects, ref. 5. For the light detected at an angle ψ the fluorescent intensities $I_{||,||}$, $I_{||,\perp}$ and $I_{\perp,||}$ are as in ref. 5 but $I_{\perp\perp}$ (see Eqn. 7 of Appendix).

$$I_{\perp\perp} = k\tfrac{1}{8}\sin^2\theta_\alpha \sin^2\theta_\varepsilon\{(1+2\cos^2\beta)+2(1-2\cos^2\beta)\sin^2\psi\} \quad (1)$$

where k is a proportionality constant, θ_α and θ_ε denote the angle between the fiber axis and the absorption and emission dipole, respectively, and β is the difference of their azimuths (Fig. 1). Fig. 3 shows the predicted limits on the values of $P_\perp$ as the angle θ_ε varies between 0 and 180°. Since angle β is in itself a function of both θ_α and θ_ε the actual value of $P_\perp$ cannot be calculated at any given θ, and only extreme possible values are shown as β varies between its allowable limits.

RESULTS

Specificity of 1,5-IAEDANS for myosin heavy chains

A typical fluorescent gel scan of electrophoretogram of skinned fibers reacted with 1,5-IAEDANS under conditions specified above is shown in Fig. 4A. The position of protein chains (indicated by arrows) were determined from an accompanying gel stained with Coomassie Blue. It is apparent that the band corresponding to heavy chains of myosin is labelled predominantly. A similar result is obtained from the electrophoretogram of myofibrils labelled with ^{3}H-labelled 1,5-IAEDANS under identical conditions and detected by looking for the presence of radioactivity in

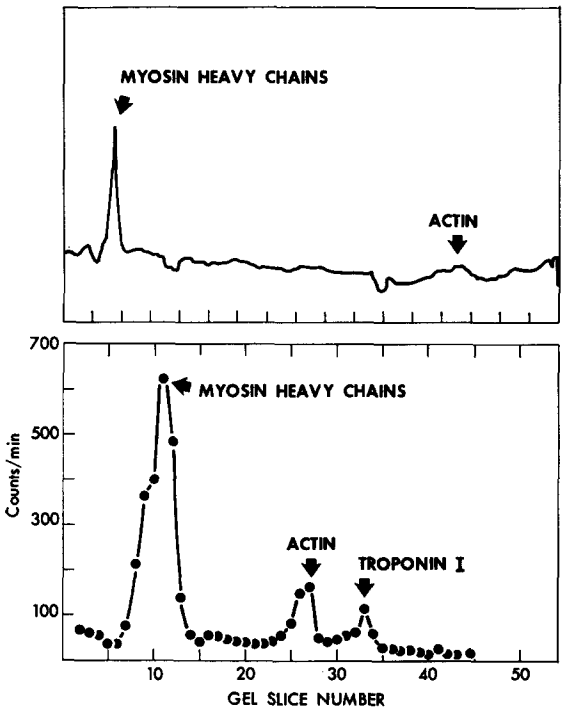

Fig. 4. Incorporation of 1,5-IAEDANS into muscle proteins. Top fluorescent scan of a microgel of a skinned glycerinated muscle fiber. Abscissa is the distance along the gel in units of 1/3 cm, ordinate the photomultiplier current in arbitrary units. Excitation and emission wavelengths were 365 and 480 nm, respectively; detection was at 0°. Bottom: distribution of radioactivity in slices of gel of myofibrils. 5 % polyacrylamide used in both cases.

separate gel slices (Fig. 4B). In particular, the relative amount of labelling of myosin with respect to actin and troponin I was 1 : 0.102 : 0.062. In this respect our technique results in an improvement over room temperature labelling of Duke et al. [10] who reported the corresponding ratios as 1 : 0.600 : 0.559. More significantly, our preparations are probably far more specifically labelled than those of Nihei et al. [3, 9] and Tregear and Mendelson [5] who carried out the reaction in the absence of ATP.

Mechanical properties of 1,5-IAEDANS-labelled fibers

In an attempt to see whether the modification of reactive thiols with 1,5-IAEDANS affected the mechanical properties of muscle we studied "rigor tension" development in native and labelled skinned single fibers. Since the mechanism of generation of rigor tension is the same as that responsible for the active force (see below), this procedure is a valid test of the physiological condition of the preparations. Maximum isometric tension could not be measured in our fibers because they usually broke a few seconds after attaining maximal contraction. Fig. 5 compares the time course of tension development in native and labelled fibers when the relaxing solution was replaced by rigor solution: no significant differences in extent of tension development were observed although modified fibers always contracted at a lower rate.

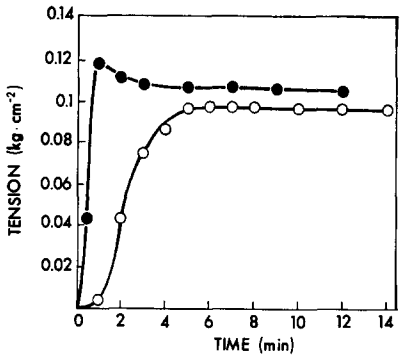

Fig. 5. The time course of rigor tension development in 1,5-IAEDANS-labelled (○) and native (●) single skinned glycerinated fibers. Fiber diameters were 70 and 74 μm, respectively. The cross-section was assumed to be circular. Relaxing solution was removed at time 0 and washing with rigor solution continued throughout the experiment.

Consistent with this finding is the fact (Borejdo, J., unpublished) that actomyosin obtained by mixing native actin with myosin which had its S_1 thiol blocked with 1,5-IAEDANS, superprecipitated to a similar extent though significantly slower than a mixture of native actin and myosin. Yamaguchi et al. [11] reported a similar effect for MalNEt-blocked rabbit skeletal myosin.

The influence of Ca^{2+} concentration in rigor solution and the effect of sarcomere length change on rigor tension for native and labelled fibers is shown in Figs. 6 and 7. Both tests failed to demonstrate a difference between the behaviors of native and modified preparations lending further support to the contention that labelling the fibers with 1,5-IAEDANS does not affect their contractility. In particular, labelled fibers are still Ca^{2+} sensitive (Fig. 6) in line with foregoing findings that neither troponin nor tropomyosin chains are reacted with the fluorophore to a considerable

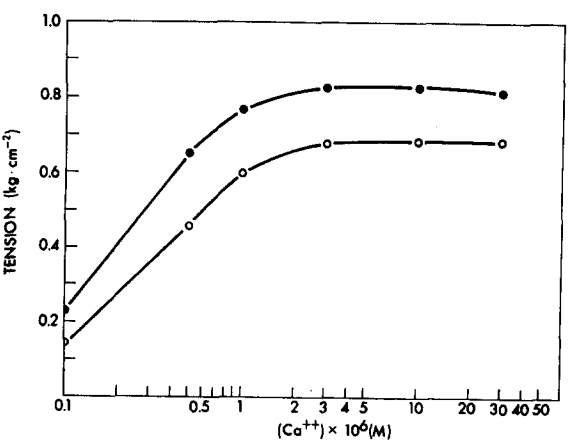

Fig. 6. Dependence of rigor tension on free Ca^{2+} concentration in rigor solution. Labelled skinned fiber (○, diameter 63 μm) and native fiber (●, diameter 60 μm). Free Ca^{2+} concentration was calculated using binding constants for Ca^{2+}-EGTA given in ref. 15.

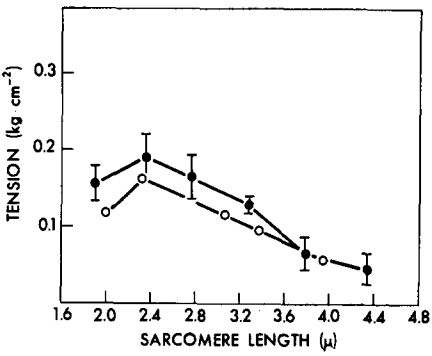

Fig. 7. The dependence of rigor tension on sarcomere length. ●, native fiber; ○, 1,5-IAEDANS-modified fiber. Error, bars (native fiber only) indicate S.D. of three measurements. Fiber diameters about 60 μm. Rigor tension induced by transferring the fiber from relaxing solution to rigor solution containing 2 mM EGTA and no added Ca^{2+}. Sarcomere length measured in the central region of the fibers under 500 × magnification.

degree. An increase in rigor force with increasing Ca^{2+} concentration in the rigor solution is expected because at higher Ca^{2+} levels force can be generated at higher ATP concentrations. This, and the fact that rigor force declines with stretch [12] (Fig. 7) support the idea that the same mechanism is involved in generation of active and rigor tension [13].

Of interest is the fact, apparent from Figs. 5, 6, and 7, that the maximum rigor tension developed by skinned single fiber is significantly lower than that usually reported for the conventional preparations [12, 13]. This is most likely associated with the increase in the rate of diffusion of ATP out of the fiber due to the absence of the cell membrane: consequently the total time during which the concentration of ATP within the fiber is low enough to render the muscle Ca^{2+} insensitive is decreased [14]. In several experiments in which the diameter of the skinned fiber was particularly small and/or the flow of washing solution rapid, the rigor tension could be as small as 0.04 kg/cm^2 or between 2 and 4 % of maximum isometric tension [12].

Polarization of fluorescence from labelled fibers in rigor and fibers irrigated with 1,5-IAEDANS heavy meromyosin.

The notation employed below is analogous to the one used by Nihei et al. [3]. The measurements were made at $\psi = \pi$. The sarcomere length along the fiber differed by less than 3 %. In spite of this uniformity, the polarization values and especially $P_\perp$ exhibited a significant variation along the length (Fig. 8). $P_\perp$ and $P_{||}$ often varied in reciprocal manner. Such variation might result from differences in the cross-sectional area which in turn lead to differences in light scattering (a depolarization source). The variations between different fibers were of the same order of magnitude and in comparing different preparations the mean polarizations from given fiber were taken. Table I summarizes the results obtained from native skinned fibers reacted directly with 1,5-IAEDANS as well as fibers irrigated with 1,5-IAEDANS-labelled heavy meromyosin at resting and extended lengths, fiber "ghosts" irrigated with labelled heavy meromyosin [14] and labelled myofibrils. It is apparent from the

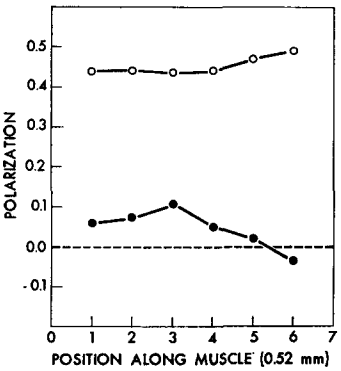

Fig. 8. Variation of polarization values along the fiber length. Typical results for a muscle in rigor ●, $P_{\perp}$; ○, $P_{||}$. Length of muscle which contributed to each determination of polarization was 520 μm.

table that while there is still a difference between the polarizations from labelled fibers and from the models meant to simulate the helical arrangement of fluorophores, viz. fibers irrigated with labelled heavy meromyosin [17], this difference is significantly smaller than previously reported [5].

Change in polarized fluorescence during rigor-relaxation cycle

Table II shows the mean values of polarized fluorescence in rigor and relaxing solutions obtained from five different fibers and measured along the line of excitation. Since skinned fibers inevitably broke during maximal isometric stimulation, the data for contracting conditions is not available. Transition from relaxation to rigor was preceded by washing the fibers with the solution containing 80 mM KCl, 5 mM

TABLE I

POLARIZATION OF FLUORESCENCE FROM LABELLED FIBERS AND MYOFIBRILS IN RIGOR, AND FROM FIBERS DECORATED WITH LABELLED HEAVY MEROMYOSIN

Mean ± S.E.; number of preparations shown at right. All preparations labelled with 1,5-IAEDANS as described in Materials and Methods. Heavy meromyosin concentration was 1.7 mg/ml. Fibers were irrigated with heavy meromyosin for 10 min, which was sufficient for saturation of all actin binding sites [7]; the excess protein was thoroughly washed out with rigor solution. The washing continued throughout the entire course of the experiment because it was noticed that background fluorescence, resulting from dissociated heavy meromyosin progressively increased with time. "Ghosts" were obtained by 10 min extraction of fibers with a modified Hasselbach-Schneider solution containing 0.6 M KCl, 10 mM sodium pyrophosphate, 2 mM $MgCl_2$, 0.1 M phosphate buffer, pH 6.4. Myofibrils consisted of an oriented bundle of about 10 single myofibrils and polarization was measured employing × 100 objective (Zeiss).

Preparation	$P_{\perp}$	$P_{||}$	n
Labelled fiber	0.076±0.008	0.462±0.003	5
Fiber+labelled heavy meromyosin	−0.018±0.024	0.474±0.013	4
Fiber ghost+labelled heavy meromyosin	0.036±0.022	0.500±0.020	3
Stretched fiber+labelled heavy meromyosin	−0.085±0.019	0.512±0.010	6
Labelled myofibrils	0.050	0.481	1

TABLE II

POLARIZATION OF FLUORESCENCE IN RIGOR AND RELAXATION

Mean ± S.E. for five measurements. The mean value of $P_\perp$ and $P_{||}$ in pyrophosphate relaxing solution (applied after relaxating solution) was 0.109 and 0.459, respectively.

State	$P_\perp$	$P_{||}$
Rigor	0.076±0.008	0.462±0.003
Relaxation	0.248±0.021	0.433±0.003

sodium pyrophosphate, 5 mM $MgCl_2$, 5 mM phosphate buffer, pH 7.0. Consequently, in this series of experiments the residual rigor tension was abolished altogether. This procedure was found to be necessary because partially contracted muscle fibers which have lost their organized sarcomere pattern contribute significantly to the artifactual depolarization of light. Thus, when measured at 370 nm single skinned glycerinated fiber produced 2.3 % depolarization of exciting light when the sarcomeres were well organized and 3.3 % depolarization when the sarcomere pattern has been lost following rigor contraction. (Rigor solution containing $3 \cdot 10^{-5}$ M Ca^{2+}, compare Fig. 5). With this procedure, transition from relaxation to rigor affected both polarization components: during relaxation both $P_\perp$ and $P_{||}$ approached the value characteristic of an assembly of random immobilized fluorophores viz. 0.35 (cf. ref. 5).

Polarization of fluorescence at different degrees of overlap

The fibers were stretched slowly in steps of about 0.1 μm per sarcomere per min. Fig. 9 shows the relationship between the polarization values measured at $\psi = \pi$ and sarcomere length in a typical experiment. While the difference between $P_\perp$ in rigor and relaxation decreased with increasing sarcomere length, it never reached zero; it is likely that this is because the rigor tension (Figs. 7 and 9) was never com-

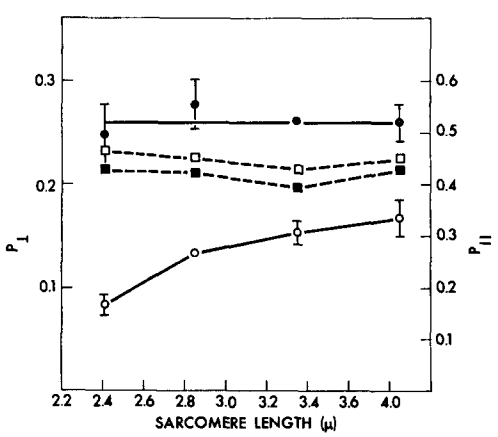

Fig. 9. The relation between the polarization values detected at angle $\psi = \pi$ from single skinned fibers and sarcomere length. $P_\perp$, circles, left scale; $P_{||}$, squares, right scale. Open symbols, rigor; filled symbols, relaxation. Sarcomere length (in the central region of the fiber) measured under 500 × magnification.

TABLE III

POLARIZATION OF FLUORESCENCE WITH 90° DETECTION SYSTEM

Mean ± S.E. Number of measurements shown at right. Resting sarcomere length was 2.2 μm, stretched length was 3.3 μm.

State	$P_\perp$	$P_{\|\|}$	n
Rigor, rest length	−0.272±0.009	0.450±0.011	6
Relaxation, rest length	−0.128±0.022	0.431±0.021	6
Rigor, stretched	−0.209±0.037	0.465±0.025	3
Relaxation, stretched	−0.131±0.012	0.439±0.011	3

pletely abolished. Within the accuracy of measurement, $P_{||}$ was insensitive to stretch both in rigor and in relaxation.

Polarization of fluorescence measured at $\psi = \pi/2$

Table III summarizes the results of six measurements from three different fiber preparations obtained at $\psi = \pi/2$. In analogy to the previous results, transition from rigor to relaxation resulted in an increase in the $P_\perp$ polarization component and in a reciprocal, though smaller change in $P_{||}$. Decreasing the amount of overlap between filaments by 78 % (50 % stretch with resting sarcomere length of 2.2 μm) resulted in little change in $P_{||}$ either in rigor or relaxation and in $P_\perp$ (relaxation) in comparison with their resting length values while $P_\perp$ (rigor) was increased. This behavior is consistent with the one shown in Fig. 9 for the $\psi = \pi$ detection of fluorescence.

DISCUSSION

For the quantitative estimation of the disposition of the cross-bridges by studying the polarized fluorescence of labelled fibers, it is essential to have at one's disposal a preparation in which only the S-1 fragment of myosin carries the fluorophore. Under our labelling conditions this requirement is closely satisfied: most of the fluorescent label is incorporated into the heavy chain of myosin and therefore into subfragment-1 [4]. The use of skinned glycerinated fibers which relax particularly well as demonstrated by their small resistance to stretch (Fig. 2), most likely due to the facilitated diffusion of the solutes [7], is in part responsible for this specificity. Furthermore, the labelling was carried out at 0 °C wherein the dissociation of actomyosin complexes is enhanced; dissociation increases the reactivity of SH_1 and depresses the reactivity of actin thiols [10].

The mechanical tests of the labelled fibers indicated that their function is not seriously impaired. Since skinned fibers broke during isometric contraction, the "rigor tension" was used as a measure of a mechanical response. Because the mechanism of generation of rigor tension is believed to be the same as that of an active force [13] the rigor tension is a valid parameter of a contractile activity of the muscle providing the replacement of relaxing solution with the rigor solution is always uniform. Furthermore, in skinned fibers the magnitude of rigor force is about 10 times smaller than the rigor force generated in whole fibers [12], owing to the rapid diffusion of ATP unhindered by the cell membrane, and it was therefore possible to

perform many reproducible rigor-relaxation cycles on a single preparation without destroying the regular pattern of sarcomere arrangement. Even though the rate of tension development was decreased in labelled fibers (Fig. 4), the maximum force was unaffected and so was the relationship between rigor force and both the free Ca^{2+} concentration (Fig. 5) and sarcomere length (Fig. 6).

The magnitudes of the polarizations detected at $\psi = \pi$ (Table I) differ systematically from the values reported earlier by Nihei et al. [3]; $P_\perp$ is always lower and $P_{||}$ larger. These differences are most likely explained in terms of the improved labelling employed presently as well as good preservation of sarcomere structure throughout the experiment, thanks to the fact that the fiber never developed more than 10% of its maximum isometric tension. The importance of preserving the sarcomere pattern was estimated by measuring the degree of depolarization of light at 370 nm by intact fibers. While it is difficult to assess quantitatively how much error would be produced by this depolarization in actual determination of $P_\perp$ and $P_{||}$, it is clear that it is significantly larger for contracted fibers, perhaps by as much as $3.3-2.3/2.3 \times 100 = 44\%$.

Comparison between the values of polarized fluorescence obtained from fibers labelled directly and from myofibrills (Table I) reveals little difference in both $P_\perp$ and $P_{||}$ which suggests that artifacts associated with light scattering by insoluble, non-myofibrillar components are negligible; however, in the experiments with myofibrills $\times$ 100 objective has been used and the collection angle was significantly increased. Thus the improvement in the quality of our sample has been obtained at the expense of accuracy of measurement and it is at present impossible to ascertain whether the lack of difference in the polarization values is real.

Upon transition from rigor to relaxation at either $\psi = \pi$ or $\psi = \pi/2$ we consistently observed a large increase in $P_\perp$ and a smaller decrease in $P_{||}$, while Nihei et al. [3] reported a small increase in $P_\perp$ and no change in $P_{||}$ employing the detection at $\psi = \pi$. These differences can also be attributed to improved labelling and preservation of sarcomere structure. It should be emphasized that in the experiments summarized in Table II, application of the rigor solution was always preceded by washing the fiber with the pyrophosphate relaxing solution and that, consequently, transition into rigor configuration was not accompanied by development of even the small "residual" rigor tension. Thus both the depolarization effects associated with the loss of organized sarcomere structure and the possible interference from the accompanying internal stresses are eliminated.

In an attempt to correlate the phenomenological changes in polarization of fluorescence with the actual angular movement of the cross-bridges Tregear and Mendelson [5] initiated an analysis which is summarized and extended in Appendix. They compared the experimental values of $P_\perp$ and $P_{||}$ with 0° detection obtained from intact fibers irrigated with the fluorophore-labelled subfragment-1 and fibers labelled directly with 1,5-IAEDANS, with the theoretically predicted values and only in the former case noted a reasonable agreement. While our data for preparations irrigated with labelled heavy meromyosin agrees closely with the values reported by Tregear and Mendelson [5] for labelled S-1, we were also able to obtain a better fit to the values of polarization predicted for directly labelled fibers in rigor in as much as that for a fixed $P_{||}$, the corresponding $P_\perp$ lies closer to the predicted value (cf. Fig. 3, ref. 5, also Appendix, Eqn. 7). The polarizations obtained from stretched fibers irrigated

with fluorescent heavy meromyosin (Table I) are in this respect closest to the theory: it is likely that by imposing internal stress in the fibers thin filaments assume more ordered (parallel) configuration and thus the assembly of fluorophores approximates an ideal helix more closely. However, by using the $\psi = \pi$ detection system we were unable to attain a full agreement with the predicted values in any of the preparations studied. In view of what was said above and since a great deal of care has been exercised during dissection and mounting, it is unlikely that this discrepancy arises from the imperfections in our experimental preparations such as twisting of the fiber or scattering by the residual membrane fragments. Thus, as first noted by Tregear and Mendelson [5] the reason for the discrepancy lies probably in the contribution to the fluorescence from randomly oriented fluorophores. In an attempt to minimize this contribution we carried out measurements with our $\psi = \pi/2$ detection system: it can be shown (see Appendix) that with detection at an angle ψ, the random contribution to the fluorescent light intensity becomes:

$$I_{\perp\perp}^{\text{random}} = k\tfrac{1}{15}[(1+2\cos^2\mu)+(1-3\cos^2\mu)\sin^2\psi] \tag{2}$$

where k is a proportionality constant and μ is the angle between the emission and absorption dipoles. With reference to Eqn. 1 and to Eqn. 2, and Eqns. 7 and 8 of Appendix and assuming equal quantum efficiencies for random and helical fluorophores $P_\perp$ measured at 90° becomes

$$P_\perp(90°) = \frac{\frac{1}{8}\sin^2\theta_\alpha \sin^2\theta_\varepsilon(3-2\cos^2\beta)-\frac{1}{2}\sin^2\theta_\alpha\cos^2\theta_\varepsilon}{\left[\frac{1}{8}\sin^2\theta_\alpha\sin^2\theta_\varepsilon(3-2\cos^2\beta)+\frac{1}{2}\sin^2\theta_\alpha\cos^2\theta_\varepsilon+\frac{2q}{1-q}\frac{1}{15}(2-\cos^2\mu)\right]} \tag{3}$$

where q is a fraction of randomly oriented fluorophores. Thus at $\psi = \pi/2$ detection, contribution from random fluorophores is minimal (though non zero). Furthermore, since the values of $P_\perp$ for fibers directly labelled with 1,5-IAEDANS and the fibers irrigated with labelled heavy meromyosin were not very much different (Table I) it is reasonable to assume as a first approximation that $q = 0$. Under those circumstances Eqn. 3 is represented by Fig. 3 and it is apparent that for the experimentally measured $P_{||}$ and associated θ_ε there exists θ_ε for which $P_\perp$ lies within its allowable limits. Thus, under those assumptions, the generalized theory of polarized fluorescence (Appendix Eqns. 7 and 8) as applied to the case of $\psi = \pi/2$ detection is self-consistent. The inclination angle which satisfies the restrictions imposed by both $P_{||}$ and $P_\perp$ through the theory outlined here lies within a narrow range $41° < \theta_\varepsilon < 42°$. During relaxation θ_ε derived from $P_{||}$ becomes closer to 42° while $P_\perp$ increases so much that a meaningful fit cannot any longer be achieved. The simplest interpretation of these results is that the helical configuration of myosin subfragment-1 moieties prevalent during rigor is largely lost in relaxation and that angle θ is no longer defined under these conditions.

In conclusion, it appears that quantitative determination of the declination of the cross-bridge in rigor is possible using $\psi = \pi/2$ detection system in skinned single fibers. We intend to take advantage of this fact in future investigation of the dynamics of the cross-bridge cycle.

APPENDIX (by R. A. Mendelson and M. F. Morales)

Here we extend and at one point correct a previous analysis [5] by R. Tregear

and one of us (R.A.M.). Referring to Fig. 1 imagine $\hat{\alpha}$ and $\hat{\varepsilon}$ to be unit vectors parallel, respectively, to the transition moments of absorption and emission of a single fluorophore located at "Obj", and let the angle between this directional doublet be $\mu = \cos^{-1}(\hat{\alpha} \cdot \hat{\varepsilon})$. Excitation (Ex) issues from "Source", and fluorescent emission (Em) is observed at "Obs". The angle between source-Obj and Obj-Obs is ψ. Our aim is to calculate the emission intensity, I, detected at Obs, along a line including $\hat{k}$ ($\|$-direction) or $\hat{n} = \hat{\imath}(-\sin\psi) + \hat{\jmath}\cos\psi$ ($\perp$-direction), in the case that the polarization plane of the excitation includes either $\hat{k}$ ($\|$-direction) or $\hat{\jmath}$ ($\perp$-direction). The expression for the intensity can be factored. The geometric factor, G_f, is the probability that a photon polarized in the Ex plane will excite oscillations in the $\hat{\alpha}$-direction times the probability that oscillations in the $\hat{\varepsilon}$-direction will produce photons polarized in the plane in which Obs chooses to detect. All other determinants of the detected I (e.g. quantum yield in the given environment, Obj-Obs distance, source and detector characteristics, etc.) are lumped into a constant, κ. In practice it is always the fluorescent emission of a population of fluorophores, say $f = 1, 2, \ldots, N$, that is detected. We will always assume that these fluorophores are non-interacting (their excitations are independent and their emissions are additive), and that they are all at the same (very large) distance from the detector, but later we will allow for environmental (therefore κ-) differences. At first we calculate I for assemblies in which the fluorophores have the same κ, but are at different spatial attitudes, i.e. differ in G_f. So we must evaluate the summation in,

$$I = \kappa \sum_{f=1}^{f=N} G_f \tag{1}$$

As discussed in the main text, our ultimate purpose is to interpret experimentally detected changes in I in terms of attitudinal transformations of the fluorophore array. Since in our idealization the fluorophores (and therefore the directional doublets) are assumed to be rigidly imbedded in the heavy meromyosin S-1 moieties of a muscle fiber, the array of heavy meromyosin S-1 moieties prescribes the array of directional doublets and vice versa. Our other studies [16, 17] suggest that an S-1 is roughly a prolate ellipsoid of revolution, and studies elsewhere have established that a thick filament is a helical array of heavy meromyosin S-1 moieties, anti-symmetrical about the M-plane and hexagonally symmetrical when projected on a transverse plane. In the state of relaxation and in the state of rigor the attitudes of the moieties are presumed to be different. We need the relation between the attitudes of the doublets ($\hat{\alpha}$, $\hat{\varepsilon}$) that determine the G_f values in Eqn. 1 and the attitudes of the heavy meromyosin S-1 moieties in the state of interest. To obtain this relation we imagine that imbedded in each heavy meromyosin S-1 is a coordinate system that takes advantage of the symmetry of the ellipsoid and that when such a moiety is placed in a reference position its imbedded system coincides with the "laboratory" system depicted in Fig. 1. In that case the components of a unit vector such as or (we shall say $\hat{v}$ for generality) will be the same in either system (Fig. 10). Now the moiety is moved to its place in the thick filament assembly corresponding to the physiological state in question, and we calculate the new, or transformed, components of $\hat{v}$ referred to the laboratory framework. This movement is a succession of rotations only, since attitudes of the imbedded doublets are invariant to translations. If, starting in the reference position, a moiety is inclined by angle η, $\hat{v}$ becomes $H(\eta) \otimes \hat{v}$; if, starting from the reference position, it is

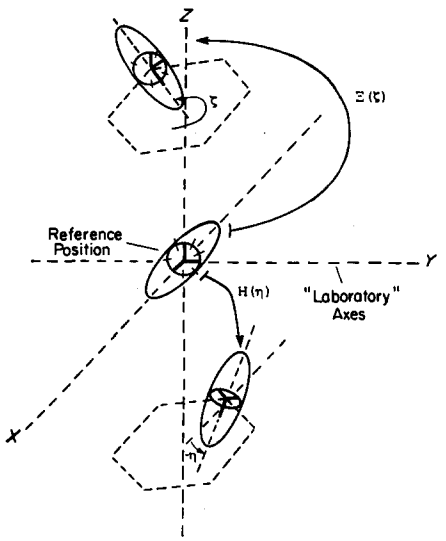

Fig. 10. Moving an S-1 moiety from a reference position to its final position in the helical array of a fiber. S-1 is assumed to be a prolate ellipsoid of revolution, and in the reference position its imbedded axes coincide with the "laboratory" axes. The imbedded unit vector, $\hat{v}$, (see text), which is not shown, maintains constant relations to the imbedded axes, but changes its relations (becomes the "transformed" $\hat{v}$) to the laboratory axes as the moiety is moved about. Pure translations of S-1 are taken for granted but require no attention. The figure illustrates two sample rotations of S-1. To reach the top position S-1 has been rotated in azimuth through angle ξ (a multiple of 60°); to reach the bottom position S-1 has been inclined by $-\eta$. The corresponding matrices are Ξ and H, respectively, i.e., these matrices multiply $\hat{v}$ to give the transformed values of $\hat{v}$.

rotated in azimuth through angle ξ, $\hat{v}$ becomes $\Xi(\xi) \otimes \hat{v}$. Here H and Ξ are non-commuting matrices of direction cosines. The antisymmetry of $N/2$ moieties on one $(+)$ side of the transverse M-plane to the $N/2$ moieties on the other $(-)$ side is expressed in certain correspondences*, $\xi^{(+)} \leftrightarrow \xi^{(-)} = -\xi^{(+)}$, and $\eta^{(+)} \leftrightarrow \eta^{(-)} = -\eta^{(+)}$. Furthermore, the hexagonal symmetry of the projection of the helix on the plane requires that $\xi = m\pi/3$; $m = 1, 2, \ldots 6$. Understanding these conditions we can say that in the array of relaxation $\hat{v}$ becomes $\Xi(\xi) \otimes \hat{v}$, and in the array of rigor $\hat{v}$ becomes $\Xi(\xi) \otimes \Xi(\zeta) \otimes H(\eta) \otimes \hat{v}$, if we allow for the (unsettled) possibility that transition from relaxation to rigor entails an azimuthal rotation through angle ζ. All the foregoing rotations preserve the condition, $\hat{\alpha} \cdot \hat{\varepsilon} = \cos \mu$, when applied to both $\hat{a}$ and $\hat{e}$. From here on we deal only with the appropriately transformed $\hat{v}$ (i.e. $\hat{\alpha}$ or $\hat{\varepsilon}$), and assume further that the components of $\hat{v}$ are expressed in spherical coordinates, φ and θ. Clearly the assembly of thick filament moieties imposes on the array of directional doublets the analogous correspondences, $\varphi^{(+)} \leftrightarrow \varphi^{(-)} = -\varphi^{(+)}$, and $\theta^{(+)} \leftrightarrow \theta^{(-)} = -\theta^{(+)}$, and the requirement, $\varphi = m\pi/3$. In the summation of Eqn. 1 these conditions would create 12 subclasses of G values, with $N/12$ fluorophores in each; however, certain circumstances and arguments will presently simplify the situation.

Identifying the absorption and emission probabilities with the squares of

* This feature was overlooked in the Tregear-Mendelson paper, and was subsequently called to our attention by Professor A. F. Huxley.

cosines of certain angles (see below, Eqn. 2), we can write the G values of a single fluorophore for the four possible experimental arrangements as,

$$\left.\begin{aligned} G_{||,||} &= (\hat{k}\cdot\hat{\alpha})^2(\hat{\varepsilon}\cdot\hat{k})^2 = \hat{\alpha}_z^2\hat{\varepsilon}_z^2 \\ G_{\perp,||} &= (\hat{\jmath}\cdot\hat{\alpha})^2(\hat{\varepsilon}\cdot\hat{k})^2 = \hat{\alpha}_y^2\hat{\varepsilon}_z^2 \\ G_{||,\perp} &= (\hat{k}\cdot\hat{\alpha})^2(\hat{\varepsilon}\cdot\hat{n})^2 = \hat{\alpha}_z^2(\hat{\varepsilon}\cdot\hat{n})^2 \\ G_{\perp,\perp} &= (\hat{\jmath}\cdot\hat{\alpha})^2(\hat{\varepsilon}\cdot\hat{n})^2 = \hat{\alpha}_y^2(\hat{\varepsilon}\cdot\hat{n})^2 \end{aligned}\right\} \tag{2}$$

If we are dealing with N fluorophores of a thick filament array, the φ and θ correspondences imply $v_x^{(+)} = v_x^{(-)}$, $v_y^{(+)} = -v_y^{(-)}$, and $v_z^{(+)} = -v_z^{(-)}$. These relations have no effect on $G_{||,||}$ and $G_{\perp,||}$, but in the expansion of $(\hat{\varepsilon}\cdot\hat{n})^2$ the cross-term, $-2\varepsilon_x\varepsilon_y\sin\psi\cos\psi$, contains ε_y and is therefore of opposite sign for the $N/2$ fluorophores to either side of the M-plane. Since the subclasses are of equal size, the cross-terms cancel out of the Eqn. 1 summation, so we simply omit them in the averaging processes to be carried out below. The condition, $\varphi = m\pi/3$ is argued away on the basis [5] that a muscle fiber is not truly crystalline, and with N so large it is probable that φ_α and φ_ε are evenly distributed in the range 0 to 2π. So, the Eqn. 1 summation over six subclasses is replaced by,

$$N\langle G_f\rangle = (N/2\pi)\int_0^{2\pi} G_f \mathrm{d}\varphi_\alpha; \qquad \hat{\alpha}\cdot\hat{\varepsilon} = \cos\mu \tag{3}$$

The ease of carrying out the averaging depends on choosing a convenient form of the μ-restraint. In the integration of Eqn. 2,

$$\beta \equiv \varphi_\alpha - \varphi_\varepsilon = \cos^{-1}\left[\frac{\cos\mu - \cos\theta_\alpha\cos\theta_\varepsilon}{\sin\theta_\alpha\sin\theta_\varepsilon}\right] \tag{4}$$

remains constant, and thus allows G_f to be expressed in terms of φ_α only. Tregear and Mendelson [5] also considered an immobile, totally disordered ("random") array of S-1 moieties (therefore of directional doublets) as a model for a damaged or unspecifically labelled fiber region; however, they derived expressions only for a special case of $\langle G(\psi = \pi)\rangle$. In order to make the general calculation it is convenient (and with $G_{||,\perp}$ and $G_{\perp,\perp}$ it is indispensable) to employ Soleillet's integration procedure and to express the μ-constraint vectorially as,

$$\hat{\varepsilon} = \hat{\alpha}\cos\mu + \left\{\frac{\hat{k} - \cos\theta_\alpha\hat{\alpha}}{\sin\theta_\alpha}\cos\gamma + \frac{\hat{\alpha}\times\hat{k}}{\sin\theta_\alpha}\sin\gamma\right\}\sin\mu \tag{5}$$

where γ measures generation angle in a cone generated by $\hat{\varepsilon}$ rotating around a fixed $\hat{\alpha}$, keeping μ constant. In this case the summation of Eqn. 1 is replaceable by,

$$N\langle G\rangle = (N/8\pi^2)\int_0^{\pi}\int_0^{2\pi}\int_0^{2\pi} G\mathrm{d}\gamma\sin\theta_\alpha\mathrm{d}\varphi_\alpha\mathrm{d}\theta_\alpha \tag{6}$$

Eqn. 5 makes it possible to express the integrand of Eqn. 6 solely in terms of γ and of $\hat{\alpha}$ quantities.

Application of Eqns. 3 and 6 to Eqn. 2 leads to the following versions of Eqn. 1, i.e. to $I/N\kappa = \langle G\rangle$:

Helical array

$$||, || \quad \alpha_z^2\varepsilon_z^2 \tag{7a}$$

$$\perp, || \quad (1/2)(1-\alpha_z^2)\varepsilon_z^2 \tag{7b}$$

$$||, \perp \quad (1/2)\alpha_z^2(1-\varepsilon_z^2) \tag{7c}$$

$$\perp, \perp \quad (1/8)(1-\alpha_z^2)(1-\varepsilon_z^2)\{(1+2\cos^2\beta)+2(1-2\cos^2\beta)\sin^2\psi\} \tag{7d}$$

Immobile, randomized array

$$||, || \quad (1/15)(1+2\cos^2\mu) \tag{8a}$$

$$\perp, || \quad (1/15)(2-\cos^2\mu) \tag{8b}$$

$$||, \perp \quad (1/15)(2-\cos^2\mu) \tag{8c}$$

$$\perp, \perp \quad (1/15)(1+2\cos^2\mu)+(1/15)(1-3\cos^2\mu)\sin^2\psi \tag{8d}$$

Because κ values are hard to estimate it is customary to report data as ratios in which κ cancels out, e.g. as simple intensity ratios [5], or as "polarization functions" such as are used in the main text:

$$P_{||} \equiv (I_{||,||}-I_{||,\perp})/(I_{||,||}+I_{||,\perp}) \tag{9}$$

$$P_{\perp} \equiv (I_{\perp,\perp}-I_{\perp,||})/(I_{\perp,\perp}+I_{\perp,||}) \tag{10}$$

From Eqns. 7 and 8 it follows that $P_{\perp}$, but not $P_{||}$, will depend on ψ. As a function of ψ, $P_{\perp}$ has a minimum at $\psi = \pi/2$, whether or not the I values are sums of contributions from "helical" and "random" arrays, each with its own N and κ so the presence of a minimum at $\psi = \pi/2$ is not diagnostic of the presence of a random array*. However, the fraction of I contributed by the random array is also minimal at $\psi = \pi/2$; so, as mentioned in the main text, "right angle observation" is preferred in practice. Minima in $P_{\perp}$ at $\psi = \pi/2$, and independence of $P_{||}$ on ψ have been experimentally observed in rigor of glycerinated fibers by one of us (R.A.M.).

ACKNOWLEDGEMENTS

We are indebted to Dr. J. Leung for assistance in assembling the experimental apparatus. This work was supported by USPHS grants HL-16683 and HL-06285, NSF grant PCM-75-22698 and AHA grant CI-8.

REFERENCES

1 Aronson, J. and Morales, M. F. (1969) Biochemistry 8, 4517–4522
2 Dos Remedios, C. G., Millikan, R. G. C. and Morales, M. F. (1972) J. Gen. Physiol. 59, 103–120
3 Nihei, T., Mendelson, R. A. and Botts, J. (1974) Biophys. J. 14, 236–242
4 Takashi, R., Duke, J., Ue, K. and Morales, M. F. (1976) Arch. Biochem. Biophys., in the press
5 Tregear, R. and Mendelson, R. A. (1975) Biophys. J. 15, 455–467
6 Szent-Gyorgyi, A. (1949) Biol. Bull. 96, 140–149

* The expression in brackets in 7d is $(1+2\cos^2\beta)$ for "straight through" ($\psi = \pi$) and $(1+2\sin^2\beta)$ for "right angle" ($\psi = \pi/2$) observation. The latter expression is erroneously given in ref. 5, p. 458.

7 Borejdo, J. and Oplatka, A. (1976) Biochim. Biophys. Acta 440, 241–258
8 Bendall, J. R. (1961) Biochem. J. 81, 520–535
9 Nihei, T., Mendelson, R. A. and Botts, J. (1974) Proc. Natl. Acad. Sci. U.S. 71, 274–277
10 Duke, J., Takashi, R., Ue, K. and Morales, M. F. (1976) Proc. Natl. Acad. Sci. U.S. 73, 302–306
11 Yamaguchi, M., Nakamura, T. and Sekine, T. (1973) Biochim. Biophys. Acta 328, 154–165
12 McGrath, P. and Dos Remedios, C. G. (1974) Experientia 30, 1036–1038
13 White, D. C. S. (1970) J. Physiol. Lond. 208, 583–605
14 Bremel, R. D. and Weber, A. (1972) Nat. New Biol. 238, 97–101
15 Chen-Lin, R. S. (1972) MSc. Thesis, Purdue University
16 Kretzschmar, M., Mendelson, R. and Morales, M. F. (1976) Biophys. Soc. Abstr. 16, 126a
17 Mendelson, R., Morales, M. F. and Botts, J. (1973) Biochemistry 12, 2250–2255